Inorganic Chemistry

Article

pubs.acs.org/IC

Synthesis and Structures of Plutonyl Nitrate Complexes: Is Plutonium Heptavalent in $PuO_3(NO_3)_2^-$?

Rémi Maurice,*[,†] Eric Renault,[‡] Yu Gong,[§] Philip X. Rutkowski,[§] and John K. Gibson*[,§]

[†]SUBATECH, UMR CNRS 6457, IN2P3/EMN Nantes/Université de Nantes, 4 rue Alfred Kastler, BP 20722, 44307 Nantes Cedex 3, France

[‡]CEISAM, UMR CNRS 6230, Université de Nantes, 2 rue de la Houssinière, BP 92208, 44322 Nantes Cedex 3, France

[§]Chemical Sciences Division, Lawrence Berkeley National Laboratory, Berkeley, California 94720, United States

Supporting Information

ABSTRACT: Gas-phase plutonium nitrate anion complexes were produced by electrospray ionization (ESI) of a plutonium nitrate solution. The ESI mass spectrum included species with all four of the common oxidation states of plutonium: Pu(III), Pu(IV), Pu(V), and Pu(VI). Plutonium nitrate complexes were isolated in a quadrupole ion trap and subjected to collision-induced dissociation (CID). CID of complexes of the general formula $PuO_x(NO_3)_y^-$ resulted in the elimination of NO_2 to produce $PuO_{x+1}(NO_3)_{y-1}^-$, which in most cases corresponds to an increase in the oxidation state of plutonium. Plutonyl species, $Pu^{V}O_2(NO_3)_2^-$ and $Pu^{VI}O_2(NO_3)_3^-$, were produced from $Pu^{III}(NO_3)_4^-$ and $Pu^{IV}(NO_3)_5^-$, respectively, by the elimination of two NO_2 molecules. CID of $Pu^{VI}O_2(NO_3)_3^-$ resulted in NO_2 elimination to yield $PuO_3(NO_3)_2^-$, in which the oxidation state of plutonium could be VII, a known oxidation state in condensed phase but not yet in the gas phase. Density functional theory confirmed the nature of $Pu^{V}O_2(NO_3)_2^-$ and $Pu^{VI}O_2(NO_3)_3^-$ as plutonyl(V/VI) cores coordinated by bidentate equatorial nitrate ligands. The computed structure of $PuO_3(NO_3)_2^-$ is essentially a plutonyl(VI) core, $Pu^{VI}O_2^{2+}$, coordinated in the equatorial plane by two nitrate ligands and one radical oxygen atom. The computations indicate that in the ground spin−orbit free state of $PuO_3(NO_3)_2^-$, the unpaired electron of the oxygen atom is antiferromagnetically coupled to the spin-triplet state of the plutonyl core. The results indicate that Pu(VII) is not a readily accessible oxidation state in the gas phase, despite that it is stable in solution and solids, but rather that a Pu(VI)-O· bonding configuration is favored, in which an oxygen radical is involved.

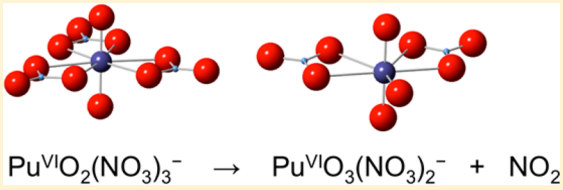

INTRODUCTION

Accessing high oxidation states of transuranic actinides, particularly plutonium, has gained much attention.[1] Hexavalent plutonium is common, primarily in the form of PuO_2^{2+} in solution. A key issue is whether it is feasible to chemically engage the $5f^2$ electrons of Pu(VI) to access higher oxidation states.[2] Krot and Gel'man first reported Pu(VII) in alkaline solution in 1967,[3] a feat shortly thereafter repeated.[4] Keller and Seiffert synthesized a solid compound containing Pu(VII).[5] More recently, Pu(VIII) has been reported in solution.[6] In the gas phase, octavalent PuO_4 has been inferred based on thermogravimetric experiments,[7] as well as from the apparent vaporization of Pu from alkaline solutions.[8] However, recent computational studies indicate that PuO_4 as a molecule comprising Pu(VIII) is not stable.[9,10] Instead, PuO_2F_4 may be a better candidate as a stable species comprising Pu(VIII).[2] In the case of Pu(VII) in the gas phase, it has been predicted that PuO_3F and Pu_2O_7 should be stable.[10] The reduction potential in solution for $Pu^{VII}O_3^+/Pu^{VI}O_2^{2+}$ is ca. +2.3 V,[1] which is only ca. 0.6 V higher than the Ce(IV/III) reduction potential; CeO_2 is a stable molecule,[11] and it might be feasible to oxidize Pu(VI) to Pu(VII) in the gas phase. An important caveat in this evaluation is that the reported Pu(VII) reduction potential is for highly basic conditions such that direct comparison of these values is not necessarily indicative of comparative intrinsic stabilities of the oxidation states.

In accord with the above assessment, the primary goal of the present work was to investigate the stability of Pu(VII) in gas-phase oxides. The decomposition of gas-phase metal nitrate anions, $M(NO_3)_n^-$, can result in the elimination of neutral NO_2, producing $MO(NO_3)_{n-1}^-$.[12−14] In cases where higher oxidation states of the metal are more accessible than that in the nitrate precursor, oxidation of the metal center can occur during these processes. An example of oxidation by elimination of NO_2, and NO, is the conversion of $Mn^{II}(NO_3)_3^-$ to $Mn^{VII}O_4^-$, in which Mn is in its highest accessible oxidation state.[14] Decomposition of plutonium nitrate anions could be a route to oxidation of Pu, possibly to Pu(VII). It is demonstrated that $PuO_x(NO_3)_y^-$ complexes do indeed lose neutral NO_2 molecules upon collision-induced dissociation (CID) in a quadrupole ion trap (QIT) resulting in oxidation of Pu, including the formation of plutonyl(V/VI) from Pu(III) and Pu(IV) complexes. Based on analogy with the proposed stable $Pu^{VII}O_3F$ molecule, it may be expected that $PuO_3(NO_3)_2^-$ would similarly comprise Pu(VII). This latter

Received: December 14, 2014
Published: February 19, 2015

DOI: 10.1021/ic502969w
Inorg. Chem. 2015, 54, 2367−2373

species was produced, and its geometric and electronic structures, including the Pu oxidation state, were evaluated by density functional theory (DFT). Moreover, the magnetic coupling constant in $PuO_3(NO_3)_2^-$ was also assessed.

EXPERIMENTAL METHODS

The experiments reported here were performed using an Agilent 6340 quadrupole ion trap mass spectrometer (QIT/MS) with the electrospray ionization (ESI) source inside a radiological contaminant glovebox, as described in detail elsewhere.[15] All the plutonium nitrate complex anions subjected to CID were produced by ESI of methanol solutions of 200 μM $Pu(NO_3)_4$. The plutonium isotope employed was Pu-242, which undergoes alpha-decay with a half-life of 3.8×10^5 y. The MS^n CID capabilities of the QIT/MS allow isolation of ions with a particular mass-to-charge ratio, m/z, and subsequent insertion of an ion−molecule reaction time without applying ion excitation. The reactions inside the ion trap occur at a temperature around 300 K.[16] In the high-resolution mode, the instrument has a detection range of 20−2200 m/z with a mass width (fwhm) of ∼0.3 m/z. Mass spectra were recorded in the negative ion accumulation and detection mode. The instrumental parameters were similar to those employed in previous experiments.[17] High-purity nitrogen gas for nebulization and drying in the ion transfer capillary was supplied from the boil-off of a liquid nitrogen Dewar. As has been discussed elsewhere,[18,19] the background water and O_2 pressure in the ion trap is estimated to be on the order of 10^{-6} Torr. The helium buffer gas pressure in the trap is constant at $\sim 10^{-4}$ Torr.

COMPUTATIONAL APPROACH

Quantum mechanical calculations have been performed on the $PuO_2(NO_3)_2^-$, $PuO_2(NO_3)_3^-$, and $PuO_3(NO_3)_2^-$ complexes to determine their molecular geometries and to characterize their electronic structures. Various isomers, which may furthermore correspond to different oxidation numbers for the Pu center, are possible, and therefore, molecular quantum mechanics is a useful tool to discriminate between the different possibilities. In order to elucidate the role of the coordination of nitrate ligands on the electronic structures of these systems, the corresponding PuO_2^+, PuO_2^{2+}, and PuO_3^+ cores have also been studied.

Geometry Optimizations. The determination of molecular geometries from quantum mechanical calculations requires the use of a given level of theory. In this work, two levels have been employed, a scalar relativistic (SR) one and another considering spin−orbit (SO) effects. The SR calculations were performed using the *Gaussian09* program package,[20] and are based on DFT. Hybrid exchange−correlation functionals lead to accurate geometries and harmonic frequencies in actinide oxides.[21] Therefore, in this work, the PBE0 exchange−correlation functional[22,23] was used, as in previous work of some of us on actinide carbides.[24] For the Pu atom, the 60-electron small-core pseudopotential ECP60MWB was considered,[25] and the remaining electrons described using a (14s13p10d8f6g)/10s9p5d4f3g segmented contracted basis set.[26] For the O and N atoms, the (12s6p3d1f)/6s3p3d1f def2-TZVPD basis sets[27,28] were used. Note that diffuse functions were considered due to the anionic nature of the ligands. Various starting geometries were considered and relaxed with local optimization algorithms. The nature of the encountered stationary points was checked by computing harmonic frequencies, and for all relevant spin configurations, the lowest energy minima were found. The spin nature of the various considered spin configurations was assessed from the $\langle S^2 \rangle$ expectation values, computed for the fictitious noninteracting systems of interest. Although no formal relationship exists between Kohn−Sham determinants and true wave functions, these expectation values are used in practice as a measure of the degree of spin state mixings. Note that the numerical grid was defined by using the *ultrafine* keyword of *Gaussian*. In order to assess the impact of SO coupling on the molecular geometries, SO−DFT calculations[29] were performed with the *NWChem* 6.3 suite of programs.[30] The exchange−correlation functional, the basis sets, and the numerical grid were chosen identical to the ones used in the SR-DFT calculations. The energy adjusted SO pseudopotential of Küchle et al.[31] was used for these calculations. In *NWChem*, the collinear approximation is used, which makes the results noninvariant with respect to rotations of the coordinate frame. Although the error in total energies can be of the order of 0.1 eV,[32] bond distances and atomic charges are not expected to be significantly dependent on the choice of the coordinate frame.

Atomic Charges and Spin Populations. In order to determine the oxidation number of the Pu atom in the studied complexes, the SR Mulliken atomic charges and spin populations of the relevant configurations of the $PuO_2(NO_3)_2^-$, $PuO_2(NO_3)_3^-$, and $PuO_3(NO_3)_2^-$ complexes were computed, as well as the SO Mulliken charges. To assess the role of the coordination of the nitrate ligands on the PuO_2^+, PuO_2^{2+}, and PuO_3^+ cores, these quantities were also determined for these uncoordinated ions. Note that in the PuO_2^+ and PuO_2^{2+} cores, the oxidation numbers of Pu are unambiguous, V and VI, respectively. Therefore, the comparison of the results obtained in the complexes and with these cores is of crucial importance to determine the oxidation numbers of Pu in the complexes. Mulliken charges are known to be basis-set dependent; therefore, the absolute values of these effective charges are not necessarily meaningful. Moreover, effective charges differ drastically from formal charges, and therefore, effective charge values alone cannot be used to assign oxidation numbers. We have chosen this charge model because it was practically available at all the levels of theory considered in this work, i.e. SR− and SO−DFT. The most important criteria concerning the oxidation number of Pu is related to atomic spin density. For high oxidation states of Pu, the Pu spin density is expected to correlate directly with the number of f electrons. Test calculations on the complexes of interest at SR levels showed that our conclusions remain valid if other charge and spin populations models are used, namely, CM5 charges[33] and Hirshfeld spin densities.[34]

Magnetic Coupling in $PuO_3(NO_3)_2^-$. As will be shown, the $PuO_3(NO_3)_2^-$ complex and the PuO_3^+ core possess two local spins at SR levels, localized on the plutonium atom i ($S_i = 1$) and on one equatorial oxygen radical j ($S_j = 1/2$). Therefore, these local spins can result in two coupled spin states, with either $S = 1/2$ or $S = 3/2$. At a given geometry, the energy difference between these two coupled spin states can be effectively described using the Heisenberg−Dirac−van Vleck Hamiltonian:[35−37]

$$\hat{H} = J\hat{S}_i \cdot \hat{S}_j$$

where J is defined as the magnetic coupling constant between the i and j magnetic centers. In this work, the SR calculations are performed within a spin-unrestricted formalism. In this case, solutions for given M_S values are obtained, and the spin quantum number S is not imposed. Here, two solutions are computed, corresponding to $M_S = 3/2$ and referred to as the high-spin (HS) solution, and the $M_S = 1/2$ solution, referred to as the spin-broken-symmetry (BS) solution. In the ideal situation of noninteracting spins (such as at the dissociation limit), the HS solution corresponds to a pure quartet spin state, and the BS solution to an ideal mixture of quartet and doublet components, for which the weights correspond to the square of Clebsch−Gordan coefficients (the BS solution would have 1/3 quartet character, and 2/3 doublet character). If one assumes that such situation is encountered, it can easily be shown that the magnetic coupling constant can be in this case extracted within this weak-coupling scheme (WCS) as follows:

$$J(\mathrm{WCS}) = E_{\mathrm{HS}} - E_{\mathrm{BS}}$$

where E_{HS} and E_{BS} correspond to the self-consistent field (SCF) energies of the HS and BS solutions, respectively. If one deviates from this ideal case, the expectation values $\langle S^2 \rangle_{\mathrm{HS}}$ and $\langle S^2 \rangle_{\mathrm{BS}}$ deviate from their ideal values (here the ideal $\langle S^2 \rangle_{\mathrm{HS}}$ value would be 15/4, and the $\langle S^2 \rangle_{\mathrm{BS}}$ value 7/4), and one may extract the magnetic coupling constant, within the intermediate coupling scheme (ICS) as proposed by Yamaguchi:[38,39]

DOI: 10.1021/ic502969w
Inorg. Chem. 2015, 54, 2367−2373

$$J(\mathrm{ICS}) = 2\frac{E_{\mathrm{HS}} - E_{\mathrm{BS}}}{\langle S^2\rangle_{\mathrm{HS}} - \langle S^2\rangle_{\mathrm{BS}}}$$

Both schemes are considered in this work, and the values obtained for both are compared.

RESULTS AND DISCUSSION

ESI of Plutonium Nitrate Solution. ESI of a nominally Pu(IV) solution resulted in a mass spectrum, displayed in Figure 1, in which it is evident that all four of the common oxidation states of plutonium are present: Pu(III), Pu(IV), Pu(V), and Pu(VI). The $Pu^{IV}(NO_3)_5^-$ and $Pu^{VI}O_2(NO_3)_3^-$ species were dominant in the ESI mass spectrum; assignments of the minor $Pu^{III}(NO_3)_4^-$ and $Pu^{IV}O(NO_3)_3^-$ peaks were confirmed from their CID spectra (see Figures S1 and S2). Unassigned peaks are attributed to impurities in the plutonium nitrate solution, which is typical under these experimental conditions.[40] Plutonium is known to coexist in its four common oxidation states in solution.[1] The ESI spectrum illustrates this distinctive phenomenon, but it should be emphasized that ESI mass spectra in general, and this one in particular, do not necessarily directly reflect solution speciation.[41]

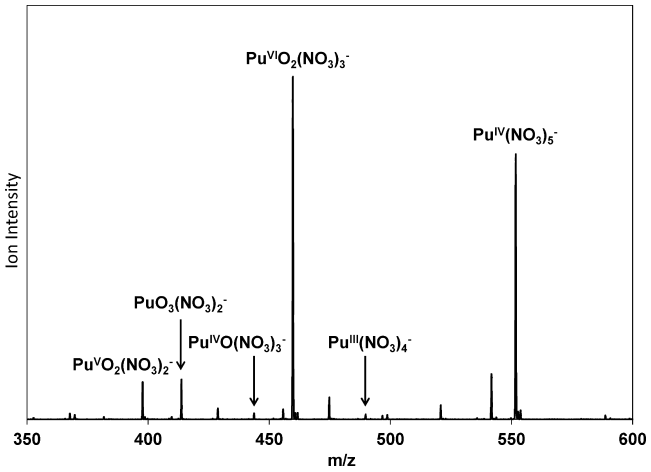

Figure 1. ESI mass spectrum of the plutonium nitrate solution. The assignments of the minor $Pu(NO_3)_4^-$ and $PuO(NO_3)_3^-$ peaks were confirmed from their CID spectra (Figures S1 and S2). CID of $Pu(NO_3)_5^-$ and $PuO_2(NO_3)_3^-$ are discussed below.

For small mononuclear metal complexes, anion ESI mass spectra are generally dominated by ions with charges of −1 or −2; only ions with the charge state −1 were observed in the present experiments. In addition to the limitation of observable charge states under these experimental conditions, there is the possibility of significant changes in speciation during ESI and ion transport into the ion trap. In the particular case of nitrate ions, facile elimination of NO_2 can result in gas-phase oxides that are not present in solution. As discussed below, fragmentation of $Pu(NO_3)_5^-$ results in $PuO_2(NO_3)_3^-$, which likely accounts for the high abundance of the latter species in the ESI mass spectrum. Despite caveats about quantitative speciation evaluations by ESI,[41] anion complexes present in solution are generally apparent in ESI mass spectra. Thus, the appearance of substantial $Pu(NO_3)_5^-$ in the ESI mass spectrum suggests that this Pu(IV) species is present in solution. In contrast, from solution speciation studies it has been suggested that $Pu(NO_3)_5^-$ is not significant at any nitrate concentration.[42] Largely based on that work, thermodynamic modeling of plutonium nitrate speciation includes neutral $Pu(NO_3)_4$ and dianionic $Pu(NO_3)_6^{2-}$, but excludes $Pu(NO_3)_5^-$.[43] There seems to be no obvious rationale as to why $Pu(NO_3)_5^-$ should not be a stable solution species—the present results show that it is a stable gas phase species that results from ESI of plutonium nitrate solutions, suggesting that its existence in solution is probable. It must be emphasized that the importance of $Pu(NO_3)_5^-$ at various nitrate concentrations (and other solution conditions) remains uncertain and furthermore that the solvent in this work was primarily methanol rather than water. However, based on the ESI results in this work, $Pu(NO_3)_5^-$ should be considered when modeling speciation in plutonium nitrate solutions.

Gas-Phase Synthesis of $PuO_x(NO_3)_y^-$. The CID spectra exhibited a variety of processes corresponding to oxidation of Pu by loss of NO_2, such as reaction 1, which are the focus of this work. Reduction processes such as by NO_3 ligand loss, reaction 2, were also observed but are not pertinent to the quest for higher oxidation states of Pu.

$$Pu^{IV}O(NO_3)_3^- \rightarrow Pu^{V}O_2(NO_3)_2^- + NO_2 \quad (1)$$

$$Pu^{VI}O_2(NO_3)_3^- \rightarrow Pu^{V}O_2(NO_3)_2^- + NO_3 \quad (2)$$

Among the observed redox processes in the CID spectra (Figures 2, 3, S1, S2) were Pu(III → IV), Pu(III → V), Pu(III → VI), Pu(IV → V), Pu(IV → VI), and Pu(VI → V). The primary motivations for this work were reactions that convert a Pu(III) or Pu(IV) nitrate anion into plutonyl, as well as the formation of a plutonium nitrate complex with an abnormally high number of oxygen atoms bonded to plutonium. The observed reactions that produce these species are presented, followed by a discussion of their geometries and electronic structures, including the Pu oxidation states. The "reactions" discussed here are induced by CID of an anionic plutonium nitrate complex that has been isolated in the ion trap and is subsequently fragmented after resonant excitation and multiple energetic collisions with helium atoms in the trap prior to acquiring the product mass spectrum. These "reactions" are thus unimolecular decompositions of the specified complex anion, not reactions with any reagent gas in the ion trap. It

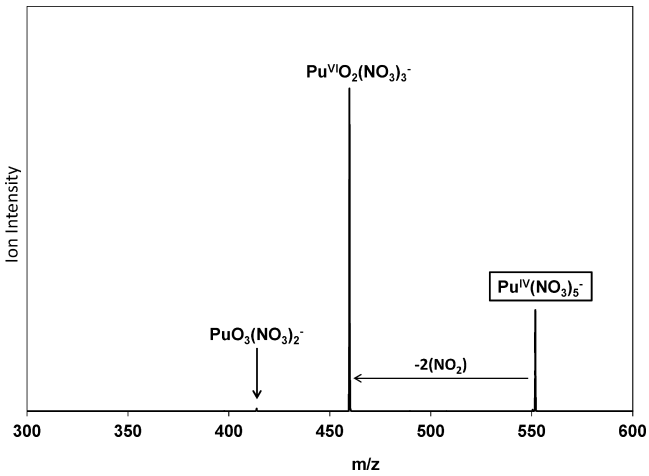

Figure 2. CID mass spectrum of $Pu(NO_3)_5^-$. The dominant channel is to produce plutonyl(VI) nitrate. A very small amount of $PuO_3(NO_3)_2^-$ is also produced, presumably by loss of a third neutral NO_2 molecule from the dominant intermediate.

DOI: 10.1021/ic502969w
Inorg. Chem. 2015, 54, 2367−2373

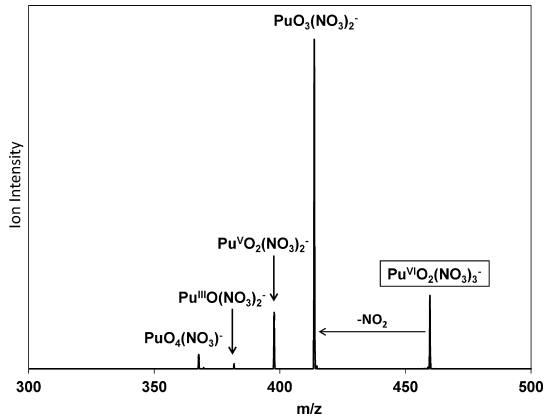

Figure 3. CID mass spectrum of $PuO_2(NO_3)_3^-$. The dominant channel is to produce $PuO_3(NO_3)_2^-$. Another significant channel is production of $PuO_2(NO_3)_2^-$.

should be remarked that the instrumental low mass limit for resonant ejection after CID precludes the identification of low m/z anion products such as NO_2^-.

The two reactions that convert plutonium nitrate complexes to plutonyl(V) and plutonyl(VI) complexes are given by reactions 3 and 4, with the corresponding CID spectra shown in Figures S1 and 2, respectively.

$$Pu^{III}(NO_3)_4^- \rightarrow Pu^{V}O_2(NO_3)_2^- + 2(NO_2) \quad (3)$$

$$Pu^{IV}(NO_3)_5^- \rightarrow Pu^{VI}O_2(NO_3)_3^- + 2(NO_2) \quad (4)$$

Rather than $2(NO_2)$, the product in reactions 3 and 4 could alternatively be N_2O_4, the formation of which is slightly less endothermic (by ca. 50 kJ/mol) but essentially degenerate in energy when ΔG at 300 K is considered.[44] There is little doubt as to the general nature and oxidation states of the plutonyl(V/VI) nitrate products in eqs 3 and 4, but their geometries and electronic structures were evaluated in detail by the computations discussed below. The ability to produce plutonyl(V) and plutonyl(VI) complexes by CID of plutonium(III) and plutonium(IV) nitrates is enabled by the low enthalpy and favorable entropy for reaction 5, and by the low reduction potentials for Pu(V/III) and Pu(VI/IV), which are both approximately 1 V.[1]

$$NO_3 \rightarrow NO_2 + O \quad (5)$$

ΔH = 211 kJ/mol[45]

The direct synthesis of plutonyl complexes from decomposition and oxidation of plutonium nitrates is significant. A second central goal of this work was to explore the possibility of further oxidizing Pu(VI) to Pu(VII) by additional loss of NO_2. As is seen in Figure 3, CID reaction 6 proceeds efficiently.

$$PuO_2(NO_3)_3^- \rightarrow PuO_3(NO_3)_2^- + NO_2 \quad (6)$$

Given that the Pu(VII/VI) reduction potential is modest, 0.85 V in basic solution,[1] it is conceivable that the product of reaction 6 is plutonium trioxide coordinated by two nitrate anions, with an oxidation state of Pu(VII). It should be emphasized that there is not necessarily a direct correlation between reduction potentials in solution, particularly basic solution, and the propensity for redox processes to occur in gas phase complexes. Solution reduction potentials cannot be employed to predict whether a gas-phase oxidation process will proceed, but they can be employed as a qualitative guide for the general feasibility of oxidation. In particular, the oxidation behavior of Pu in basic solution does not necessarily indicate that the Pu(VII) oxidation state should be similarly accessible in the gas phase, but it does suggest this as a reasonable target. An alternative structure is plutonyl(V) nitrate coordinated by an oxygen radical to yield an oxidation state of Pu(VI). This latter scenario is seen in such species as $CaO(NO_3)_2^-$, where the Ca(III) oxidation state is essentially inaccessible.[14] Also apparent in Figure 3 is a small peak that corresponds to $PuO_4(NO_3)^-$, which could conceivably be Pu(VIII) tetraoxide coordinated by a nitrate. However, the octavalent oxidation state is less viable than Pu(VII) and it has furthermore been convincingly demonstrated by theory that the oxidation state in the neutral PuO_4 core is not even Pu(VI), but rather remarkably only Pu(V): $(PuO_2^+)(O_2^-)$.[9] The computed molecular geometries and electronic structures of $Pu^{V}O_2(NO_3)_2^-$, $Pu^{VI}O_2(NO_3)_3^-$, and $PuO_3(NO_3)_2^-$ are presented below. As the nomenclature of the first two of these species suggests, they could confidently be assigned as plutonyl(V) and plutonyl(VI) nitrates, which is confirmed and elaborated by the theory results below. The nature of $PuO_3(NO_3)_2^-$ is not similarly apparent and computations were needed to characterize this exotic species.

Molecular Geometries. The optimized geometries shown in Figure 4 for the $PuO_2(NO_3)_2^-$ (left), $PuO_2(NO_3)_3^-$ (middle), and $PuO_3(NO_3)_2^-$ (right) complexes correspond to M_S values of 3/2, 1, and 3/2 respectively. Note that the ground spin configuration of the $PuO_3(NO_3)_2^-$ complex is the same as one of the bare PuO_3^+ ions (i.e., M_S = 1/2). It is known from multiconfigurational-wave-function-based calculations that the ground spin state of the plutonyl PuO_2^+ core is a quartet,[46] and the one of the plutonyl PuO_2^{2+} core is a triplet.[47,48] Thus, the present DFT calculations are in agreement with these results. Because for the $PuO_3(NO_3)_2^-$ complex and the PuO_3^+ core, the ground M_S = 1/2 configurations do not correspond to pure spin states ($\langle S^2 \rangle \geq 1.74$ and $\langle S^2 \rangle \geq 1.72$, respectively), but rather to a BS solution (see the Electronic Structures section), the higher-energy HS geometry, which is similar to the ground BS geometry while more physically grounded, is also reported, and used for the calculation of the magnetic coupling constants as discussed below. The HS configuration is only 123 meV (12 kJ/mol) higher in energy than the BS configuration at the HS geometry (see the Magnetic Coupling section). The optimal geometries of the $PuO_2(NO_3)_2^-$ and $PuO_2(NO_3)_3^-$ complexes, as well as the geometry of the HS solution for $PuO_3(NO_3)_2^-$, are shown in Figure 4, and the most relevant geometrical parameters are reported in Table 1 (see Table S1 for the PuO_2^+, PuO_2^{2+}, and PuO_3^+ cores). In all the considered complexes, a linear O−Pu−O arrangement is observed, whereas the other fragments (nitrates or oxygen) are located

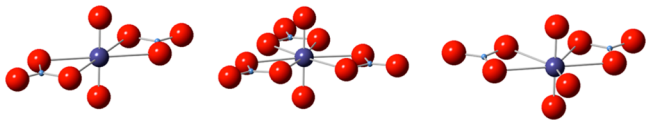

Figure 4. Ball and stick representations of the $PuO_2(NO_3)_2^-$ (left), $PuO_2(NO_3)_3^-$ (middle), and $PuO_3(NO_3)_2^-$ (right) complexes. For the $PuO_3(NO_3)_2^-$ complex, the high-spin (HS) configuration geometry is shown, the ground spin-broken-symmetry (BS) state one being practically the same. Color code: Pu (violet), O (red), and N (blue).

DOI: 10.1021/ic502969w
Inorg. Chem. 2015, 54, 2367−2373

Table 1. Scalar-Relativistic Geometrical Parameters of the $PuO_2(NO_3)_2^-$, $PuO_2(NO_3)_3^-$, and $PuO_3(NO_3)_2^-$ Complexes

complex	$d(Pu-O_{1,2})^a$ (Å)	$\alpha(O_1-Pu-O_2)^a$ (deg)	$d(Pu-O_3)^b$ (Å)
$PuO_2(NO_3)_2^-$	1.75	180.0	N/A
$PuO_2(NO_3)_3^-$	1.71	179.8	N/A
$PuO_3(NO_3)_2^-$ (HS)	1.72	178.7	2.12
$PuO_3(NO_3)_2^-$ (BS)	1.72	179.9	2.08

[a] O_1 and O_2 correspond to the oxygen atoms of the plutonyl units. [b] O_3 corresponds to the oxygen atom that does not belong to a plutonyl or nitrate unit.

in the equatorial plane, with much longer Pu−O distances than for those oxygen atoms in the axial orientation. The structure of the PuO_3^+ core is unusual in that it consists of a linear plutonyl moiety with the third oxygen atom in the equatorial plane. Note that a geometry of the $PuO_2(NO_3)_3^-$ complex has been recently computed by Odoh and Schreckenbach[49] and that the geometry obtained in this work is in very good agreement with their reported structure. For all three of the complexes studied here, the axial Pu−O distances are close to 1.7 Å, which is typical for plutonyl units. Coordination by equatorial nitrate ligands slightly destabilizes the Pu−O bonds (see the distances reported in Tables 1 and S1). Although all the converged geometries strictly belong to the C_1 symmetry point group, the $PuO_2(NO_3)_2^-$ geometry can be considered as D_{2h} symmetry, while the $PuO_2(NO_3)_3^-$ and $PuO_3(NO_3)_2^-$ complexes are close to C_{3h} symmetry and C_{2v} symmetry, respectively. For all the studied systems, the SO−DFT geometries (see Table S2) are in good agreement with the SR−DFT ones (see Tables 1 and S1), with only a slight shortening of the Pu−O equatorial bond in $PuO_3(NO_3)_2^-$. However, this change is not expected to modify the oxidation number of the plutonium center (see the following section), such that only the SR results are reported in the main text.

Electronic Structures. In order to further describe the electronic structure of these systems, Mulliken atomic charges and spin populations were computed (see Tables 2 and S7). In the $PuO_2(NO_3)_2^-$ complex, as in the PuO_2^+ core, the Pu atom possess three unpaired electrons, which indicates a Pu(V) oxidation state. Note that in the PuO_2^+ core, these unpaired electrons are located on nonbonding δ_u and ϕ_u f orbitals of the Pu atom.[46] In the $PuO_2(NO_3)_3^-$ complex, as well as in the PuO_2^{2+} core, two unpaired electrons are associated with the Pu atom, which corresponds to a Pu(VI) oxidation state. In the PuO_2^{2+} core, due to the use of a single-determinental picture, SR-DFT leads to a δ_u^2 electronic structure instead of the $\delta_u^1\phi_u^1$ one.[47,48,50,51] The δ_u and ϕ_u levels being nonbonding in this core, this does not affect much computed geometries, atomic charges and atomic spin densities, which are the important quantities reported in this work. However, in order to simplify the discussion and avoid confusion, the Kohn−Sham orbitals bearing the unpaired electrons are not plotted. In the $PuO_3(NO_3)_2^-$ complex (for both the HS and BS geometries), two unpaired electrons are associated with the Pu atom, whereas the effective Pu charge is very close to that in the $PuO_2(NO_3)_3^-$ complex. Moreover, the "lone" oxygen atom, $\mathbf{O_3}$, has one unpaired electron, either coupled ferromagnetically to the plutonyl triplet (HS solution) or antiferromagnetically (BS solution). The same behavior is obtained for the PuO_3^+ core. Therefore, it is concluded that the Pu atom is not further oxidized in the $PuO_3(NO_3)_2^-$ complex compared with $PuO_2(NO_3)_3^-$, that is, the plutonium oxidation state is Pu(VI), not Pu(VII), in the $PuO_3(NO_3)_2^-$ complex. From these results, one can easily understand that the SO coupling cannot significantly affect the molecular geometries of these plutony systems, because it essentially mixes the ground SO free configuration with configurations that belong to the same electronic configuration, or with configurations that only differ by the occupation of the essentially nonbonding f orbitals of the Pu center. For instance, in the $PuO_2(NO_3)_2^-$ case, as in the PuO_2^+ core, the $\phi_u^2\delta_u^1$ and $\phi_u^1\delta_u^2$ configurations are coupled and mixed in the ground SO state due to SO coupling (with quartet and doublet spin components), whereas in $PuO_2(NO_3)_3^-$, as in PuO_2^{2+}, the ground SO state, obtained from multiconfigurational wave function calculations, is found to be essentially constituted of the $\phi_u^1\delta_u^1$ configuration[46] (with triplet and singlet spin components). In the $PuO_3(NO_3)_2^-$ complex, the lowest energy doublet and quartet components are expected to be mixed by SO coupling. These components correspond to a similar electronic structure, with two unpaired electrons on the Pu center, and one unpaired electron on the oxygen radical. For similar reasons, the atomic charges are hardly affected by SO coupling (see Tables 2, S1, and S8), and therefore, the qualitative conclusions concerning the oxidation states of the Pu centers in these nitrate complexes are independent of the introduction of SO coupling. However, one should note that the SO coupling breaks the spin symmetry and that its proper inclusion would result in a quartet/doublet mixture in the ground SO state of the $PuO_2(NO_3)_2^-$ and $PuO_3(NO_3)_2^-$ systems (and also in the corresponding PuO_2^+ and PuO_3^+ cores), as well as in a triplet/singlet mixture in the $PuO_2(NO_3)_3^-$ complex (and in the PuO_2^{2+} core). The numerical determination of these mixtures can be obtained from two-step SO approaches within a multiconfigurational framework, as done by La Macchia et al. in the PuO_2^+ and PuO_2^{2+} cores.[46] However, this task is beyond the scope of the present work, which focuses on the molecular geometries and oxidation states of the synthesized plutonyl nitrate complexes.

Table 2. Scalar-Relativistic Mulliken Atomic Charges (q) and Atomic Spin Populations (μ) of the $PuO_2(NO_3)_2^-$, $PuO_2(NO_3)_3^-$, and $PuO_3(NO_3)_2^-$ Complexes

complex	Pu		$O_{1,2}{}^a$		$O_3{}^b$	
	q (e)	μ (e^-)	q (e)	μ (e^-)	q (e)	μ (e^-)
$PuO_2(NO_3)_2^-$	1.78	3.41	−0.67	−0.18	N/A	N/A
$PuO_2(NO_3)_3^-$	2.37	2.38	−0.66	−0.15	N/A	N/A
$PuO_3(NO_3)_2^-$ (HS)	2.34	2.29	−0.64	−0.12	−0.61	0.98
$PuO_3(NO_3)_2^-$ (BS)	2.31	2.45	−0.65	−0.18	−0.57	−1.05

[a] O_1 and O_2 correspond to the oxygen atoms of the plutonyl units. Computed values for O_1 and O_2 differ by less than 0.01 in all the reported cases. [b] O_3 corresponds to the oxygen atom that does not belong to any plutonyl or nitrate unit.

DOI: 10.1021/ic502969w
Inorg. Chem. 2015, 54, 2367−2373

Magnetic Coupling in $PuO_3(NO_3)_2^-$. To extend our SR-DFT study, the magnetic coupling constant in the $PuO_3(NO_3)_2^-$ complex was computed for the HS geometry. From the results shown in Table 3, we obtain a J value of 123 meV with both the WCS and the ICS coupling schemes. These values are practically identical, which is not surprising given that the computed values of $<S^2>_{HS}$ and $<S^2>_{BS}$ are very close to the ideal ones of the WCS (3.75 and 1.75, respectively). Therefore, it is concluded that an oxygen radical is present in the $PuO_3(NO_3)_2^-$ complex and that its unpaired electron is antiferromagnetically coupled to plutonium, with a large coupling constant. Therefore, the ground SO free state is a spin doublet, and the ground SO state is predicted to have a dominant doublet character. Indeed, due to the absence of an inversion center, the doublet and quartet components mix under the effect of SO coupling, which is often referred to as antisymmetric exchange or Dzyaloshinskii–Moriya interaction.[52−54] By comparing Tables 2 and S9, one can see that the magnetic coupling constant is strongly affected by the coordination of equatorial nitrate ligands. This parameter is known to be strongly dependent on the geometry, and it should be noted that the smaller coupling value in the $PuO_3(NO_3)_2^-$ complex is associated with a larger Pu–O_3 distance than in the PuO_3^+ core.

Table 3. Energy Difference between the High-Spin (HS) and Spin-Broken-Symmetry (BS) Configurations of the $PuO_3(NO_3)_2^-$ Complex (HS Geometry) and $<S^2>$ Values for the HS and BS Configurations, Respectively

parameter	value
$E_{HS} - E_{BS}$ (meV)	123
$<S^2>_{HS}$	3.78
$<S^2>_{BS}$	1.77

CONCLUSIONS

ESI of a nominally plutonium(IV) nitrate solution resulted in species corresponding to the four readily accessible oxidation states of plutonium: Pu(III), Pu(IV), Pu(V), and Pu(VI). Although changes in oxidation state can occur during ESI, which is an electrochemical process, the coexistence of these four oxidation states is consistent with solution chemistry and the known low reduction potentials for Pu(VI), Pu(V), and Pu(IV). A dominant species in the ESI mass spectrum was $Pu^{IV}(NO_3)_5^-$, which is generally not considered a significant solution species. Recognizing that ESI mass spectra do not directly represent solution speciation, this result nonetheless suggests that $Pu^{IV}(NO_3)_5^-$ should be considered when modeling plutonium nitrate solution speciation. CID-induced NO_2 elimination from $Pu^{III}(NO_3)_4^-$ and $Pu^{IV}(NO_3)_5^-$ resulted in $Pu^{V}O_2(NO_3)_2^-$ and $Pu^{VI}O_2(NO_3)_3^-$, respectively, demonstrating the direct synthesis of plutonyl from plutonium nitrate. CID of $Pu^{VI}O_2(NO_3)_3^-$ resulted in loss of an additional NO_2 molecule to produce $PuO_3(NO_2)_2^-$; it was postulated that this species could have a PuO_3^+ core in which the oxidation state is Pu(VII), an oxidation state known to exist in solution. However, DFT computations revealed that the structure of the PuO_3^+ core in $PuO_3(NO_2)_2^-$ is similar to that of the PuO_2^{2+} core in $PuO_2(NO_3)_3^-$, with an oxidation state of Pu(VI) in both. The $PuO_3(NO_2)_2^-$ complex can be represented as PuO_2^{2+} coordinated in the equatorial plane by two nitrate ligands and one radical oxygen atom. The results indicate that Pu(VI) is not readily oxidized to Pu(VII) in the gas phase, as might have been expected, but rather that a species comprising a radical oxygen atom bound to Pu(VI) is the more favorable bonding configuration.

ASSOCIATED CONTENT

Supporting Information

CID mass spectra of $Pu(NO_3)_4^-$ and $PuO(NO_3)_3^-$. SR geometrical parameters of the bare PuO_2^+, PuO_2^{2+}, and PuO_3^+ ions; SR and SO geometrical parameters of the bare ions and of the complexes; SR molecular geometries of the $PuO_2(NO_3)_2^-$, $PuO_2(NO_3)_3^-$, and $PuO_3(NO_3)_2^-$ plutonium nitrate complexes; SR Mulliken atomic charges and atomic spin populations of the bare PuO_2^+, PuO_2^{2+}, and PuO_3^+ ions; SO Mulliken atomic charges of the bare ions and of the complexes; and energy difference between the HS and BS configurations of the bare PuO_3^+ ion (HS geometry) and $<S^2>$ values for the HS and BS configurations, respectively. This material is available free of charge via the Internet at http://pubs.acs.org.

AUTHOR INFORMATION

Corresponding Authors

*E-mail: remi.maurice@subatech.in2p3.fr.
*E-mail: jkgibson@lbl.gov.

Notes

The authors declare no competing financial interest.

ACKNOWLEDGMENTS

The work of Y.G., P.X.R., and J.K.G. was fully supported by the U.S. Department of Energy, Office of Basic Energy Sciences, Heavy Element Chemistry, at LBNL under Contract No. DE-AC02-05CH11231.

REFERENCES

(1) Clark, D. L.; Hecker, S. S.; Jarvinen, G. D.; Neu, M. P. In *The Chemistry of the Actinide and Transactinide Elements*; 3rd ed.; Morss, L. R., Edelstein, N. M., Fuger, J., Eds.; Springer: Dordrecht, The Netherlands, 2006; Vol. 2, pp 813–1264.
(2) Dyall, K. G. *Chem. Phys.* **2005**, *311*, 19–24.
(3) Krot, N. N.; Gel'man, A. D. *Dokl. Akad. Nauk SSSR* **1967**, *177*, 124–126.
(4) Spitsyn, V. I.; Gel'man, A. D.; Krot, N. N.; Mefodiye, M. P.; Zakharov, F. A.; Komkov, Y. A.; Shilov, V. P.; Smirnova, I. V. *J. Inorg. Nucl. Chem.* **1969**, *31*, 2733–2745.
(5) Keller, C.; Seiffert, H. *Angew. Chem., Int. Ed.* **1969**, *8*, 279–280.
(6) Tananaev, I. G.; Nikonov, M. V.; Myasoedov, B. F.; Clark, D. L. *J. Alloys Compd.* **2007**, *444*, 668–672.
(7) Domanov, V. P.; Lobanov, Y. V. *Radiochemistry* **2009**, *51*, 14–17.
(8) Nikonov, M. V.; Kiselev, Y. M.; Tananaev, I. G.; Myasoedov, B. F. *Dokl. Chem.* **2011**, *437*, 69–71.
(9) Huang, W.; Xu, W. H.; Su, J.; Schwarz, W. H. E.; Li, J. *Inorg. Chem.* **2013**, *52*, 14237–14245.
(10) Zaitsevskii, A. V.; Titov, A. V.; Mal'kov, S. S.; Tananaev, I. G.; Kiselev, Y. M. *Dokl. Chem.* **2013**, *448*, 1–3.
(11) Gabelnick, S. D.; Reedy, G. T.; Chasanov, M. G. *J. Chem. Phys.* **1974**, *60*, 1167–1171.
(12) Li, F. M.; Byers, M. A.; Houk, R. S. *J. Am. Soc. Mass Spectrom.* **2003**, *14*, 671–679.
(13) Schröder, D.; de Jong, K. P.; Roithová, J. *Eur. J. Inorg. Chem.* **2009**, 2121–2128.
(14) Franski, R.; Sobieszczuk, K.; Gierczyk, B. *Int. J. Mass Spectrom.* **2014**, *369*, 98–104.
(15) Rios, D.; Rutkowski, P. X.; Shuh, D. K.; Bray, T. H.; Gibson, J. K.; Van Stipdonk, M. J. *J. Mass Spectrom* **2011**, *46*, 1247–1254.
(16) Gronert, S. *J. Am. Soc. Mass Spectrom.* **1998**, *9*, 845–848.

DOI: 10.1021/ic502969w
Inorg. Chem. 2015, 54, 2367–2373

(17) Gong, Y.; Gibson, J. K. *J. Phys. Chem. A* **2013**, *117*, 783−787.
(18) Rutkowski, P. X.; Michelini, M. C.; Bray, T. H.; Russo, N.; Marçalo, J.; Gibson, J. K. *Theor. Chem. Acc.* **2011**, *129*, 575−592.
(19) Rios, D.; Michelini, M. C.; Lucena, A. F.; Marçalo, J.; Bray, T. H.; Gibson, J. K. *Inorg. Chem.* **2012**, *51*, 6603−6614.
(20) Frisch, M. J. et al. *Gaussian 2009*, Revision D.01; Gaussian, Inc.: Wallingford, CT, 2013.
(21) Kovacs, A.; Konings, R. J. M. *J. Phys. Chem. A* **2011**, *115*, 6646−6656.
(22) Perdew, J. P.; Emzerhof, M.; Burke, K. *J. Chem. Phys.* **1996**, *105*, 9982−9985.
(23) Adamo, C.; Barone, V. *J. Chem. Phys.* **1999**, *110*, 6158−6170.
(24) Pereira, C. C. L.; Maurice, R.; Lucena, A. F.; Hu, S. X.; Gonçalves, A. P.; Marçalo, J.; Gibson, J. K.; Andrews, L.; Gagliardi, L. *Inorg. Chem.* **2013**, *52*, 10968−10975.
(25) Cao, X. Y.; Dolg, M.; Stoll, H. *J. Chem. Phys.* **2003**, *118*, 487−496.
(26) Cao, X. Y.; Dolg, M. *J. Mol. Struct.: THEOCHEM* **2004**, *673*, 203−209.
(27) Weigend, F.; Ahlrichs, R. *Phys. Chem. Chem. Phys.* **2005**, *7*, 3297−3305.
(28) Rappoport, D.; Furche, F. *J. Chem. Phys.* **2010**, 133.
(29) Nichols, P.; Govind, N.; Bylaska, E. J.; de Jong, W. A. *J. Chem. Theory Comput* **2009**, *5*, 491−499.
(30) Valiev, M.; Bylaska, E. J.; Govind, N.; Kowalski, K.; Straatsma, T. P.; Van Dam, H. J. J.; Wang, D.; Nieplocha, J.; Apra, E.; Windus, T. L.; de Jong, W. *Comput. Phys. Commun.* **2010**, *181*, 1477−1489.
(31) Küchle, W.; Dolg, M.; Stoll, H.; Preuss, H. *J. Chem. Phys.* **1994**, *100*, 7535−7542.
(32) van Wüllen, C. *J. Comput. Chem.* **2002**, *23*, 779−785.
(33) Marenich, A. V.; Jerome, S. V.; Cramer, C. J.; Truhlar, D. G. *J. Chem. Theory Comput* **2012**, *8*, 527−541.
(34) Hirshfeld, F. L. *Theor. Chim. Acta* **1977**, *44*, 129−138.
(35) Heisenberg, W. *Z. Phys.* **1928**, *49*, 619−636.
(36) Dirac, P. A. M. *Proc. Royal Soc. London* **1929**, *123*, 714−733.
(37) van Vleck, J. H. *Rev. Mod. Phys.* **1945**, *17*, 27−47.
(38) Yamaguchi, K. *Chem. Phys. Lett.* **1975**, *33*, 330−335.
(39) Yamaguchi, K.; Fukui, H.; Fueno, T. *Chem. Lett.* **1986**, 625−628.
(40) Rios, D.; Rutkowski, P. X.; Van Stipdonk, M. J.; Gibson, J. K. *Inorg. Chem.* **2011**, *50*, 4781−4790.
(41) McDonald, L. W.; Campbell, J. A.; Clark, S. B. *Anal. Chem.* **2014**, *86*, 1023−1029.
(42) Veirs, D. K.; Smith, C. A.; Berg, J. M.; Zwick, B. D.; Marsh, S. F.; Allen, P.; Conradson, S. D. *J. Alloys Compd.* **1994**, *213*, 328−332.
(43) Kubic, W. L.; Jackson, J. C. *J. Radioanal. Nucl. Chem.* **2012**, *293*, 601−612.
(44) Lias, S. G.; Bartmess, J. E.; Liebman, J. F.; Holmes, J. L.; Levin, R. D.; Mallard, W. G. In *NIST Chemistry WebBook, NIST Standard Reference Database Number 69*; Linstrom, P. J., Mallard, W. G., Eds.; National Institue of Standards and Technology: Gaithersburg, MD, 2014.
(45) Lias, S. G.; Bartmess, J. E.; Liebman, J. F.; Holmes, J. L.; Levin, R. D.; Mallard, W. G. *J. Phys. Chem. Ref. Data* **1988**, *17*, 1−861.
(46) La Macchia, G.; Infante, I.; Raab, J.; Gibson, J. K.; Gagliardi, L. *Phys. Chem. Chem. Phys.* **2008**, *10*, 7278−7283.
(47) Ismail, N.; Heully, J. L.; Saue, T.; Daudey, J. P.; Marsden, C. J. *Chem. Phys. Lett.* **1999**, *300*, 296−302.
(48) Gendron, F.; Pritchard, B.; Bolvin, H.; Autschbach, J. *Inorg. Chem.* **2014**, *53*, 8577−8592.
(49) Odoh, S. O.; Schreckenbach, G. *J. Phys. Chem. A* **2011**, *115*, 14110−14119.
(50) Craw, J. S.; Vincent, M. A.; Hillier, I. H.; Wallwork, A. L. *J. Phys. Chem.* **1995**, *99*, 10181−10185.
(51) Hay, P. J.; Martin, R. L.; Schreckenbach, G. *J. Phys. Chem. A* **2000**, *104*, 6259−6270.
(52) Dzyaloshinsky, I. *J. Phys. Chem. Solids* **1958**, *4*, 241−255.
(53) Moriya, T. *Phys. Rev.* **1960**, *120*, 91−98.
(54) Maurice, R.; de Graaf, C.; Guihery, N. *Phys. Chem. Chem. Phys.* **2013**, *15*, 18784−18804.

DOI: 10.1021/ic502969w
Inorg. Chem. 2015, 54, 2367−2373